

Application of close-range remote sensing for automatic identification of ice jams in rivers in the area of the inlet to the fishway

Jan Błotnicki¹, Maciej Gruszczyński², Paweł Jarzembowski³, Marcin Popczyk⁴✉

¹  <https://orcid.org/0000-0001-7286-0710>

²  <https://orcid.org/0000-0003-3663-2723>

³  <https://orcid.org/0000-0002-7869-7763>

⁴  <https://orcid.org/0000-0002-0814-7838>

^{1,2} Wrocław University of Environmental and Life Sciences, Institute of Environmental Engineering
Wrocław, Poland

³ Wrocław University of Environmental and Life Sciences, Department of Plant Biology
Institute of Environmental Biology, Wrocław, Poland

⁴ Silesian University of Technology

Faculty of Mining, Safety Engineering and Industrial Automation, Gliwice, Poland

e-mail: {¹jan.blotnicki; ²maciej.gruszczyński; ³pawel.jarzembowski}@upwr.edu.pl

⁴marcin.popczyk@polsl.pl

✉ corresponding author

Keywords: UAV, ice jam, frazil ice, remote sensing, frazil ice jam, fish pass, fish passage, fish ladder

JEL Classification: Q54, C53, C55, C61

Abstract

Ice phenomena in watercourses and channels pose a threat to flow continuity and hydrotechnical devices. The organoleptic method, relying on human observation, has limitations such as a narrow range, subjective assessment, and high effort, leading to its decline in use. This article presents a number of modern techniques, i.e., the interpretation of RGB images, using unmanned aerial vehicles. Drone imagery offers a bird's-eye view of areas that would otherwise be difficult to survey. It can improve the detection of frazil ice jams and, thus, contribute to the monitoring and spread of frazil ice. The authors performed research in the area of the Wrocław Water Junction on the Odra River in the area of the inlet near the fish pass at the Opatowice Weir during the flow of frazil ice on the water surface. To observe the phenomenon, a UAV with an RGB camera was used to record video in an orthogonal perspective in order to reduce geometric distortions of the optical system. The center of the frame was used for the analysis. The presented research results and the recognition of the literature indicate the possibility of using the presented technique for early detection of a potential threat from emerging ice phenomena. The results of the conducted analyses are objectively compared to the observational technique used at observation stations and allow for a reliable comparison of the intensity of ice phenomena in selected periods.

Introduction

The ice cover in inland waters is formed as a result of water cooling to a temperature close to zero. In Polish conditions, the ice usually forms at the turn of fall and winter due to intense heat radiation from the water surface and its cooling. In the

heat balance, the dominant factors are the short-wave radiation of the sun and the long-wave radiation of the water surface. Considering the above facts, it should be expected that, during cloudless and frosty nights, the first ice crystals will form in the supercooled water (Kostrzewski & Majewski, 2021).

Ice jams are a major problem in cold regions on waterways around the world. The ice that forms in them can lead to blockages that can impede the flow of traffic and even cause significant damage in places where dams and other structures are located. Whether ice phenomena occur in a particular intensity or frequency is particularly dependent on the climatic conditions and the nature of their course (Łukaszewicz & Jawgiel, 2017). The air temperature is the primary factor that determines the formation of ice phenomena in a river. It is the course of atmospheric circulation that regulates the course of the ice phenomena on a river since it influences the variability of water thermals and, consequently, a variety of forms of ice form on the river (Ptak, Choiński & Kirviel, 2016; Łukaszewicz, 2017).

Various observation and data analysis techniques are employed to identify ice phenomena relating to frazil ice. Researchers utilize methods such as aerial image analysis (Zhang et al., 2021), field measurements (McFarlane, Loewen & Hicks, 2019), ice observation with cameras on buoys (Rogers et al., 2016), satellite observations (Ito et al., 2015), and numerical modeling (Svensson & Omstedt, 1998). Image analysis enables the identification of morphological characteristics of frazil ice, such as size, shape, and concentration. Field measurements allow for direct observation of processes occurring on the water surface and an assessment of ice distribution. Satellite data provides information on ice distribution on a large spatial scale, enabling monitoring and forecasting of frazil ice-related hazards over a larger area. Numerical methods, such as hydrodynamic models and simulation models, allow for the simulation and prediction of frazil ice behavior based on various factors, such as temperature, flow velocity, and water chemistry.

An unmanned aerial vehicle (UAV), commonly known as a drone or remotely piloted aircraft (RPAS), is an aircraft without a pilot on board. The combination of the platform, control segment, and

payload is sometimes referred to as an unmanned aerial system (UAS), although the terms are used interchangeably. The use of aircraft for agricultural purposes dates back to the 19th century. The first recorded case in 1860 used balloons to take pictures for remote sensing purposes. In 1903, cameras mounted on the breasts of pigeons were used (Shelare et al., 2021). Currently, drones are widely used in the civil and commercial sectors, from precision farming, environmental monitoring, archaeology, geodesy, and mining to rescue operations or transport of goods (Rogers et al., 2016). The ability of drones to seamlessly carry sensors continues to transform workflows, push the boundaries of traditional techniques, and generate insights into new and innovative ways. In scientific articles on the use of UAVs and frazil ice, the authors focus on building a machine learning system that enables segmentation of ice sheets on the river within the limits of external conditions. However, there are no complicated and free tools to measure the speed of floating ice. The aim of this work is to develop a methodology to detect and measure the flow rate of frazil ice.

Literature review

As the flow of ice moves through a river, the particles are called frazil ice (i.e., ice slush) and are almost always the first ice to form in rivers. As a result of the cold air forcing open-water areas to become slightly below the freezing point of water, and as the water becomes slightly supercooled, ice crystals begin to form in the water. The movement of the water can result in the formation of frazil ice if there is sufficient turbulent movement in the water (Figure 1) so the ice crystals can mix with the water below the water's surface (Mattke & Gulliver, 1994).

Frazil ice occurs with the participation of the sample's suspension with crystallization nuclei (e.g., fine grains of clay) so that ice crystals become

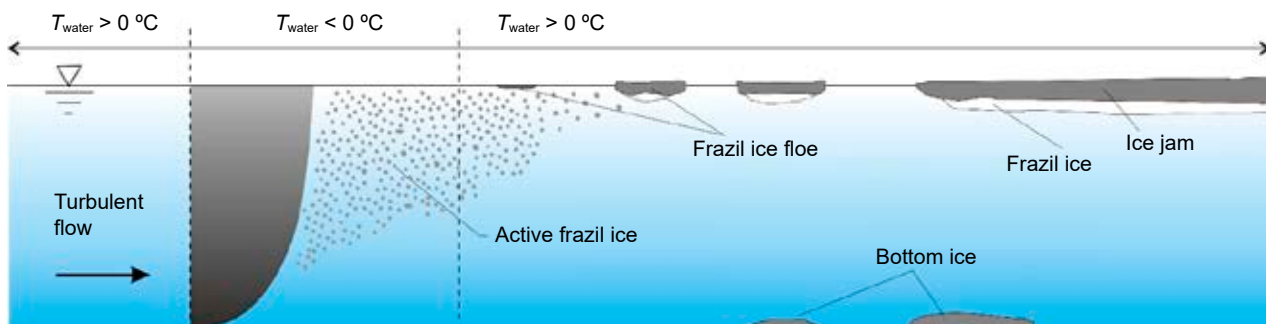


Figure 1. Forming of frazil ice based on Kolerski (2014)

visible – both in the entire volume of water and at the bottom. They are usually about a millimeter or smaller in size and typically resemble thin disks in shape. As a part of the initial ice formation process, frazil ice appears in several different forms: (1) thin, sheet-like formations (at very low current velocities); (2) particles that flocculate into larger masses of water and resemble slushy appearance on top of the water; (3) frazil masses that have irregular shapes, which appear to be shallow at first glance but are somewhat deeper than they appear on the surface, and; (4) a mixture of ice particles that are dispersed throughout the flow (at high current velocities) (Ashton, 2007). The most prevalent form of frazil ice involves characteristic spongy ice discs, which can increase in diameter from 30 cm to even as high as 3 meters (Figure 2). Their white, slightly raised edges define their characteristics, resulting from the collisions of the discs with each other.

The particles in the frazil ice adhere to each other due to the supercooling of river water. Even though the supercooling may only be a few hundredths of a degree Celsius or less, this is enough to cause the ice particles to grow and stick together in the supercooled water. When the particles contact a surface that is cooled below the freezing point, they freeze and adhere to the surface. The formation of frazil ice can also be associated with hydrotechnical facilities. When the discharge of a spillway is effectively mixed with the outside air, and the water temperature in the reservoir reaches the freezing point, the

spillway can produce a significant amount of frazil ice in winter. When a spillway is crossed, enormous amounts of frazil ice can form, which may then be deposited downstream, possibly creating a frazil ice jam (Mattke & Gulliver, 1994).

In rivers and streams, frazil particles may also adhere to the bottom and build up a loose, porous layer known as anchor ice. There can be considerable head reductions across hydroelectric dams as a result of anchor ice on the riverbed, which is caused by a supercooled water column (Jasek et al., 2015; Pan, Shen & Jasek, 2020).

If the active frazil ice is carried under an ice sheet, it can adhere to the sheet bottom, blocking a part of the flow area to create a hanging dam. The resulting problems can be significant. This phenomenon can cause problems at hydraulic structures (Beltaos, 1983) where frazil ice particles can accumulate, and when forming ice jams and blocking the intake of water (Kempema & Ettema, 2016), interfering with shipping operations in both freshwater and saline waters (Daly, 2013), affecting the bridge pier scour (Hou et al., 2022), low-dam weir, and hydropower plants (Rădoane, Ciaglic & Rădoane, 2010; Gebre et al., 2013), or even altering fish activity and habitats (Brown, 2000; Stickler et al., 2010; Brown, Hubert & Daly, 2011). During the spring breakup of the ice cover at the end of winter, and even to a lesser degree during the freeze-up period of the current winter, the jamming of rivers can result as a consequence of ice cover formation (Reimnitz, 2002).



Figure 2. Photograph of the research site taken with a UAV with a marked fishway (12/02/2021)

To enable fish to overcome damming, passages commonly known as fish passes or fishways are created (Mokwa, 2010; Safta, Petica & Mándera, 2018; Clay, 2019; Radecki-Pawlik et al., 2019), which are the most effective solution so far (Song et al., 2019). They are carried out to facilitate and restore fish migration in both directions and biological continuity along the river in the conditions of damming up the hydrotechnical facility (Schilt, 2007; Pelicice, Pompeu & Agostinho, 2015; Shi et al., 2015; Kim et al., 2016; Stamou et al., 2018; Plesinski, Gibbins & Radecki-Pawlik, 2019). Figure 2 depicts a study site near a hydrotechnical weir, where a fishway is installed.

Due to the described properties, flowing frazil ice poses a direct and indirect threat to fish. Directly, frazil ice in the current in supercooled water is dangerous for fish because it can stick to their gills, which in many situations contributes to their death (Kolerski, 2014). An indirect threat relates to the partial or complete blocking of the migration route by the deposition of ice on the partitions of the fish passes. Figure 2 shows the ice cover on the fishway pier that, similar to water intakes or other water structures, is susceptible to ice accretion caused by the transport of frazil ice. Settling ice can cause a reduction in the active flow field and, thus, affect depths and velocities. Changing the hydraulic conditions is an undesirable phenomenon due to the emerging deviation from the parameters designed for the fish pass of expected fish species. Increasing the average or maximum velocities may exceed the

swimming capabilities of the fish and, thus, prevent migration.

Materials

The research was carried out on 12/02/2021 directly in front of the Opatowice Weir located in km 245+035 of the course of the Odra River in Wrocław (Poland), which is a part of the Bartoszowice-Opatowice barrage, consisting of two weirs and two locks (Figure 3). This barrage is an important element of the canalized Odra River and performs three main functions: (1) it maintains permanent damming on weirs for navigation purposes, (2) stabilizes ground and water conditions for agricultural and forestry purposes, and (3) stabilizes the riverbed. At this barrage, with the help of the Bartoszowice Opatowice weirs, the waters are divided into the City Odra River and the Flood Canal, as well as supplying the Bartoszowice-Zacisze Navigation Canal. The Opatowice weir consists of three spans with a clearance of 32 m each, separated by pillars. The normal damming level (NPP) at the Opatowice Weir is 117.70 m NN. The bottom water level is 115.65 m NN, which is maintained for the needs of the Śródmiejski Węzeł Wodny power plant in Wrocław. A fishway is installed at the weir, which allows migration up and down the river.

The research was conducted via UAV DJI Mavic Air 2, equipped with an RGB camera. Table 1 shows the exact specifications of the camera and drone.



Figure 3. Area of interest (based on Open Street Map)

Table 1. Specifications of the DJI Mavic Air 2 camera

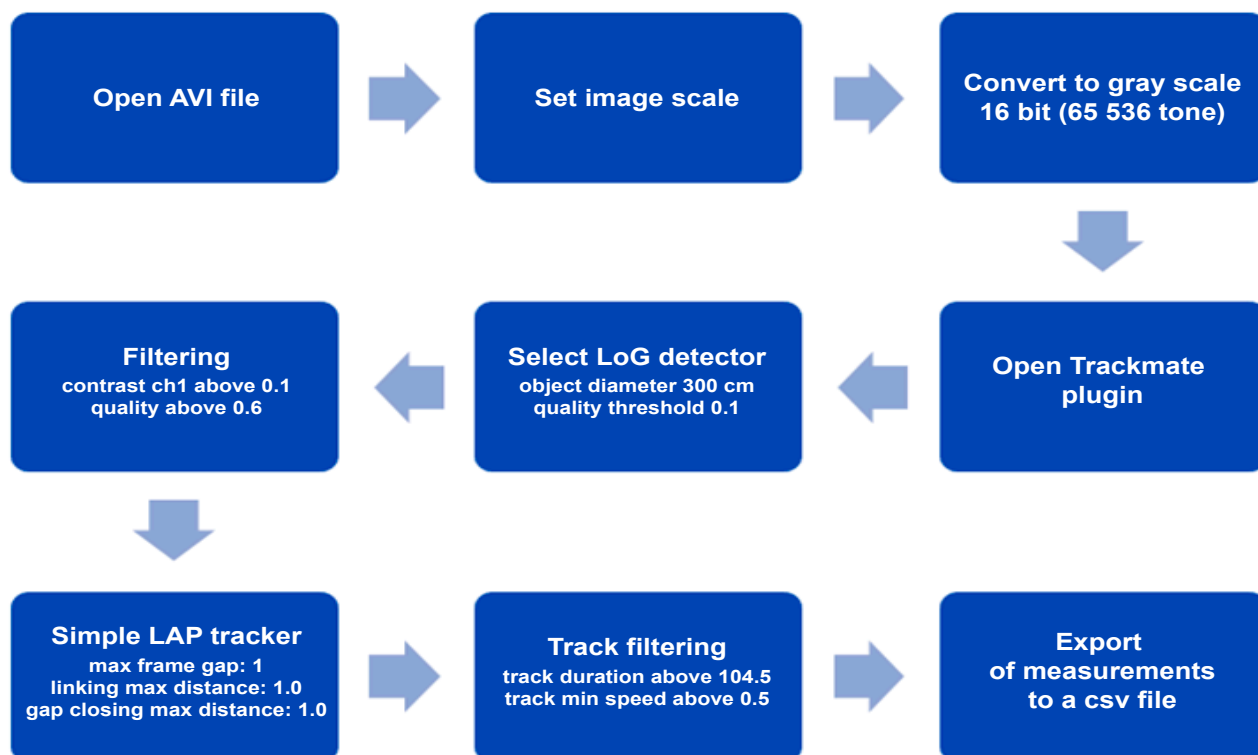
Main unit	Dimensions	183×253×77 mm
	Weight	570 g
RGB camera	Camera type	12MP, 1/2" CMOS
	Image size	4000×3000 pixels
	Shutter release	Rolling shutter
	Lens	f/2.8; 4.5/24 mm, FOV 84°
	Additional features	Internal motion unit (IMU), magnetometer
Video properties	Video resolution	1920×1080 pixels
	Video frame rates	29.97 fps
	Color profiles	Normal
	Ground sampling distance (GSD)	7.5 cm/px

Methodology

For the analysis of the average speed of frazil ice, we used an open-source Fiji version 1.53t (Schindelin et al., 2012) and plugin TrackMate (Ershov et al., 2021). We build optimal experimental setups to rapidly process and analyze the recordings. TrackMate extracts the X and Y positions of the floating ice for each frame. This information allows us to generate moving trajectories, calculate moving distances, and determine preference indices

in two-choice assays. Notably, this free-cost analysis method does not require a high ability to handle programs or scripting.

The video recording from the drone was converted to avi format, supported by the Fiji program. The imported file was converted to greyscale and calibrated on the X and Y axes. In the Fiji program, the TrackMate plugin was chosen, in which the LoG detection algorithm was selected. This detector applies a LoG (Laplacian of Gaussian) filter to the image, with a sigma suited to the blob estimated size (Lowe, 2004). Calculations are made in Fourier space. The maxima in the filtered image are searched for, and maxima too close to each other were suppressed. A quadratic fitting scheme enabled sub-pixel localization (Ershov et al., 2021). Algorithm parameters were set to an object diameter of 300 cm and a quality threshold of 0.1. Then, the objects were filtered with two filters: contrast on the first channel (single-channel grayscale image) and based on the quality $Q \geq 0.28$. The initial thresholding was set as 0. Next, the LAP tracker algorithm with the following parameters was selected for tracking the movement: max frame gap: 1; alternative linking cost factor: 1.05; linking max distance: 1.0; gap closing max distance: 1.0; splitting max distance: 15.0; cutoff percentile: 0.9. This tracker is identical to the sparse LAP tracker present in the TrackMate, except that

**Figure 4. Workflow diagram for the Fiji and TrackMate plugin**

it proposes fewer tuning options. Namely, only gap closing is allowed based solely on distance and time conditions. Track splitting and merging were not allowed, resulting in having non-branching tracks. This tracker is based on the mathematical framework known as the linear assignment problem. Its implementation is adapted from the following paper: Robust single-particle tracking in live-cell time-lapse sequences (Jaqaman et al., 2008). Tracking occurs in two steps: first, spots are linked from frame to frame to build track segments. These track segments are investigated in a second step for gap-closing (missing detection), splitting, and merging events. Linking costs are proportional to the square distance between the source and target spots, which makes this tracker suitable for Brownian motion. Solving the LAP relies on the Jonker-Volgenant solver and a sparse cost matrix formulation, allowing it to handle very large problems (Tinevez et al., 2017). Tracks were selected for further research, where the scope of observation covered the entire recording, and there were no gaps in the track. The entire image processing process is graphically presented in Figure 4. Bearing in mind the linear movement of the ice, the maximum distance function was used as the total distance traveled. This made it possible to eliminate local reading errors resulting from the compression of the video material.

In addition to the displacement and average velocity, a coefficient called the confinement ratio and the mean directional change were also calculated. The confinement ratio indicates how efficient the track was to move relative to the starting point. This is a unitless value ranging from 0 to 1. Values close to 0 indicate that the object was moving close to the starting point. Values close to 1 signify that the object is moving along the line (De Pascalis et al., 2018). The mean directional change rate measures the angle between two succeeding links or points, averaged over all the links of a single track. Statistical details are mentioned in the Figure and Table captions. The normality of the distributions was assessed by the Shapiro-Wilk W test (Shapiro & Wilk, 1965), where $p \leq 0.05$ rejected normal distribution. Data analysis was performed using the software program R (R Core Team, 2019) and R Studio (RStudio Team, 2019).

Results

During the analysis, the recorded ice drifting algorithm tracked 77 tracks continuously in 6.41 seconds on a surface with dimensions 86×70 m (see

Figures 5 and 6). The initial number of traces was larger. However, some data was filtered out due to discontinuity of observations, a low-quality factor, and outliers (basic statistics are shown in Table 2). Except for average distance and speed, the data is not normally distributed. The average track displacement is 3.779 m (standard deviation, sd, of 0.3887) at an average speed of 0.5911 m/s (sd = 0.0606). A high confinement ratio (mean = 0.9458) and low standard range of deviation (0.0782) indicate a highly linear nature of ice movement, undisturbed by current turbulence and possible water eddies (see Figure 7). The mean directional change rate readings are low; after converting radians to degrees, the average change is about 24° (mean = 0.4553 and sd = 0.2173). Considering the noise generated by the camera's matrix compression algorithm and the relatively low video resolution, the factor may be even lower.

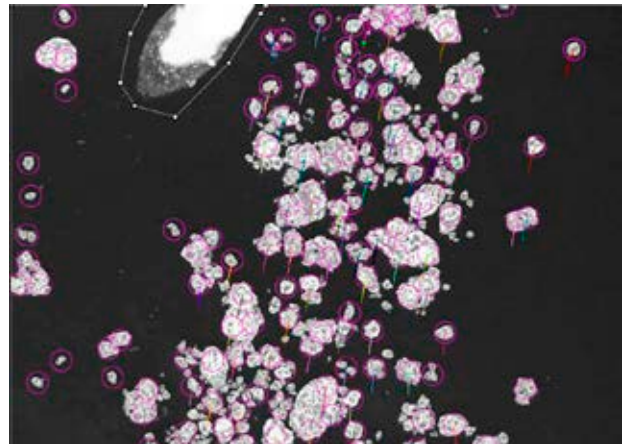


Figure 5. Film frame with a frazil ice flow. Tracking points are marked with a purple circle and the colored lines are the distance traveled

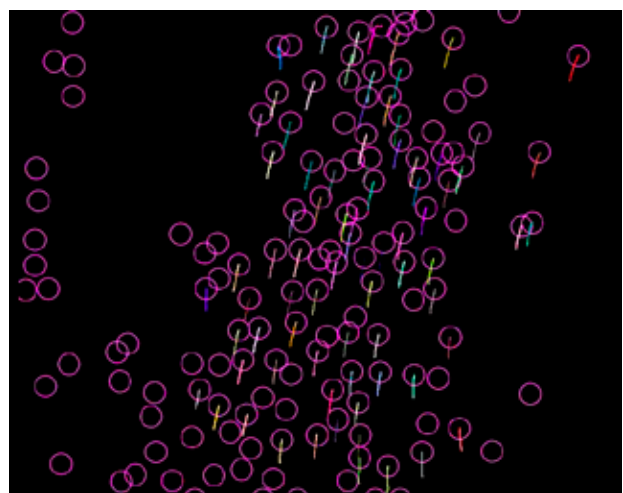
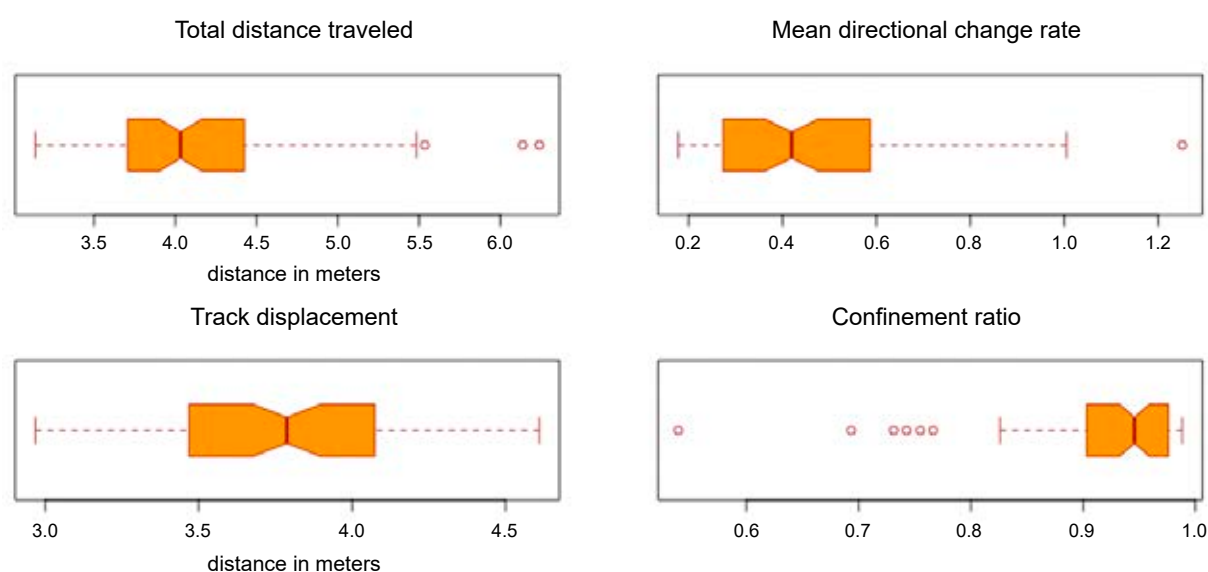


Figure 6. Film frame with the source layer removed. Visible spots, circle radii, and paths depict tracking of the movements

Table 2. Descriptive statistics for the variables

	Track displacement	Track speed (m/s)	Total distance traveled	Confinement ratio	Mean directional change rate
Minimum	2.968	0.463	3.14	0.5392	0.1179
1st quartile	3.47	0.5414	3.714	0.9034	0.2754
Median	3.787	0.5909	4.033	0.9458	0.4192
Mean	3.779	0.5895	4.122	0.9246	0.4553
3rd quartile	4.073	0.6354	4.402	0.9759	0.5862
Maximum	4.61	0.7192	6.24	0.9884	1.2512
SD	0.3887	0.0606	0.5965	0.0782	0.2173

**Figure 7. Boxplots of total distance traveled, track displacement, mean directional change rate, and confinement ratio**

Summary and conclusions

The presented method is used to detect frazil ice (and observe its area and shape) to enable early detection of ice aggregations. Observation of the average velocity enables early detection of congestion. The use of drone (UAV) overflights in the orthogonal view of the observed area and from a relatively low height allows us to achieve a much higher resolution compared to the resolution obtained from satellite, radar, or drone overflight data; for example, in work by Zhang et al. (2021), where the photographs were taken without orthorectification. The presented innovative technique, after implementation, allows for an effective prevention of the formation of ice jams. Based on experience, the services operating hydrotechnical devices know which areas of watercourses are at risk of blockages; the technique presented in the publication is dedicated to these areas. The proposed solution is a local view of an area at risk, not a global risk assessment for the entire river.

Accordingly, the most effective tool to prevent congestion is to observe the average speed and the area in the frame.

TrackMate is optimized for bright, round objects against a dark background. This means that videos with a low frame rate (or recorded in difficult lighting conditions) may be inaccurately analyzed with the plugin. It can be helpful to use the filter (i.e., a Gaussian filter) or lower the color depth to 16 or 8 bits. In extreme cases, image binarization is helpful. The possibility of scripting the open-source code of the application enables an adjustment of the parameters of the trackers to your needs. The performance of the various trackers implemented in TrackMate was measured using data from the ISBI Particle Tracking Challenge (Chenouard et al., 2014). The use of the TrackMate plugin and the Internet of Things (IoT) will enable the creation of a low-cost system for assessing the speed of ice and detecting ice jams. Data processing depends on the size of the video file and the performance of the hardware.

With the use of an office computer, obtaining data is possible after one minute. Quickly obtained results can protect against disasters because they can help detect and prevent problems before they escalate into more serious issues. The limitation of the method is the need to locate a high-quality camera over the observed area and to obtain good-quality photos, which is not always possible due to weather conditions. Currently, our methodology requires processing the collected data in a non-automatic way since the proposed technique is in a developmental (not the implementation) phase. The suggested methodology will be developed towards achieving automatic threat detection and prediction of the level of danger for a hydrotechnical facility.

References

- ASHTON, G.D. (2007) *Ice in Lakes and Rivers*. Encyclopædia Britannica. [Online]. Available from: <https://www.britannica.com/science/lake-ice/Ice-in-rivers> [Accessed: January 01, 2023].
- BELTAOS, S. (1983) River ice jams: Theory, case studies, and applications. *Journal of Hydraulic Engineering* 109(10), pp. 1338–1359, doi: 10.1061/(ASCE)0733-9429(1983)109:10(1338).
- BROWN, R. (2000) Effects of hanging ice dams on winter movements and swimming activity of fish. *Journal of Fish Biology* 57(5), pp. 1150–1159, doi: 10.1006/jfbi.2000.1378.
- BROWN, R.S., HUBERT, W.A. & DALY, S.F. (2011) A primer on winter, ice, and fish: What fisheries biologists should know about winter ice processes and stream-dwelling fish. *Fisheries* 36(1), pp. 8–26, doi: 10.1577/03632415.2011.10389052.
- CHENOUEARD, N. et al. (2014) Objective comparison of particle tracking methods. *Nature Methods* 11(3), pp. 281–289, doi: 10.1038/nmeth.2808.
- CLAY, C.H. (2019) *Design of Fishways and Other Fish Facilities*. 2nd Edition. CRC Press, doi: 10.1201/9781315141046.
- DALY, S.F. (2013) Frazil ice. In: S. Beltaos (ed.) *River Ice Formation. Committee on River Ice Processes and the Environment*. Edmonton, Alberta, pp. 107–134.
- DE PASCALIS, C., PÉREZ-GONZÁLEZ, C., SEETHARAMAN, S., BOËDA, B., VIANAY, B., BURUTE, M., LEDUC, C., BORCHI, N., TREPAT, X. & ETIENNE-MANNEVILLE, S. (2018) Intermediate filaments control collective migration by restricting traction forces and sustaining cell–cell contacts. *Journal of Cell Biology* 217(9), pp. 3031–3044, doi: 10.1083/jcb.201801162.
- ERSHOV, D., PHAN, M.-S., PYLVÄNÄINEN, J.W., RIGAUD, S.U., LE BLANC, L., CHARLES-ORSZAG, A., CONWAY, J.R.W., LAINE, R.F., ROY, N.H., BONAZZI, D., DUMÉNIL, G., JACQUEMET, G. & TINEVEZ, J.-Y. (2021) Bringing TrackMate in the era of machine-learning and deep-learning. *bioRxiv*, doi: 10.1101/2021.09.03.458852.
- GEBRE, S.B., ALFREDSEN, K., LIA, L., STICKLER, M. & TESAKER, E. (2013) Review of ice effects on hydropower systems. *Journal of Cold Regions Engineering*, 27(4), pp. 196–222, doi: 10.1061/(ASCE)CR.1943-5495.0000059.
- HOU, Z., WANG, J., SUI, J., SONG, F. & LI, Z. (2022) Impact of local scour around a bridge pier on migration of wavel-shape accumulation of ice particles under an ice cover. *Water* 14(14), 2193, doi: 10.3390/w14142193.
- ITO, M., OHSHIMA, K.I., FUKAMACHI, Y., SIMIZU, D., IWAMOTO, K., MATSUMURA, Y., MAHONEY, A.R. & EICKEN, H. (2015) Observations of supercooled water and frazil ice formation in an Arctic coastal polynya from moorings and satellite imagery. *Annals of Glaciology* 56(69), pp. 307–314, doi: 10.3189/2015AoG69A839.
- JAQAMAN, K., LOERKE, D., METTLEN, M., KUWATA, H., GRINSTEIN, S., SCHMID, S.L. & DANUSER, G. (2008) Robust single-particle tracking in live-cell time-lapse sequences. *Nature Methods* 5(8), pp. 695–702, doi: 10.1038/nmeth.1237.
- JASEK, M., SHEN, H.T., PAN, J. & PASLAWSKI, K. (2015) Anchor ice waves and their impact on winter ice cover stability. *Proceedings of the 18th Workshop on the Hydraulics of Ice Covered Rivers*, Quebec City, Canada.
- KEMPENA, E.W. & ETTEMA, R. (2016) Fish, ice, and wedge-wire screen water intakes. *Journal of Cold Regions Engineering* 30(2), doi: 10.1061/(ASCE)CR.1943-5495.0000097.
- KIM, J.-H., YOON, J.-D., BAEK, S.-H., PARK, S.-H., LEE, J.-W., LEE, A.-A. & JANG, M.-H. (2016) An efficiency analysis of a nature-like fishway for freshwater fish ascending a large Korean river. *Water* 8(1), 3, doi: 10.3390/w8010003.
- KOLERSKI, T. (2014) *Ochrona przed powodziami zatorowymi na Dolnej Odrze i jeziorze Dąbie*. Gdańsk.
- KOSTRZEWSKI, A. & MAJEWSKI, M. (Eds) (2021) *Zintegrowany Monitoring Środowiska Przyrodniczego. Organizacja, system pomiarowy, metody badań. Wytuczne do realizacji*. Warszawa: Główny Inspektorat Ochrony Środowiska.
- LOWE, D.G. (2004) Distinctive image features from scale-invariant keypoints. *International Journal of Computer Vision* 60(2), pp. 91–110, doi: 10.1023/B:VISI.0000029664.99615.94.
- Łukaszewicz, J. (2017) Przebieg i charakter zjawisk lodowych na wybranych odcinkach rzek Przymorza o wysokim stopniu antropopresji na tle zmian klimatycznych zachodzących w strefie brzegowej Bałtyku. *Acta Scientiarum Polonorum – Architectura Budownictwo* 16(1), pp. 93–113, doi: 10.22630/ASPA.2017.16.1.09.
- Łukaszewicz, T.J. & JAWGIEL, K. (2017) Zmienność częstości i charakteru przebiegu zjawisk lodowych na rzece Parsęcie w aspekcie zmian klimatycznych. *Badania Fizjograficzne, Geografia Fizyczna* 68(1954), pp. 79–98, doi: 10.14746/bfg.2017.8.6.
- MATTKE, T.W. & GULLIVER, J.S. (1994) *Ice Jam Formation Processes*. St. Paul, Minnesota.
- McFARLANE, V., LOEWEN, M. & HICKS, F. (2019) Field measurements of suspended frazil ice. Part II: Observations and analyses of frazil ice properties during the principal and residual supercooling phases. *Cold Regions Science and Technology* 165, doi: 10.1016/j.coldregions.2019.102796.
- MOKWA, M. (2010) Hydraulic calculations for fishways. *Acta Scientiarum Polonorum. Formatio Circumiectus* 9(2), pp. 43–48 (in Polish).
- PAN, J., SHEN, H.T. & JASEK, M. (2020) Anchor ice effects on river hydraulics. *Cold Regions Science and Technology* 174, 103062, doi: 10.1016/j.coldregions.2020.103062.
- PELICICE, F.M., POMPEU, P.S. & AGOSTINHO, A.A. (2015) Large reservoirs as ecological barriers to downstream movements of Neotropical migratory fish. *Fish and Fisheries* 16(4), pp. 697–715, doi: 10.1111/faf.12089.
- PLESINSKI, K., GIBBINS, C.N. & RADECKI-PAWLIK, A. (2019) Effects of interlocked carpet ramps on upstream movement of brown trout (*Salmo trutta*) in an upland stream. *Journal of Ecohydraulics* 5(5), doi: 10.1080/24705357.2019.1581102.

28. PTAK, M., CHOIŃSKI, A. & KIRVIEL, J. (2016) Long-term water temperature fluctuations in coastal rivers (southern Baltic) in Poland. *Bulletin of Geography. Physical Geography Series* 11(1), pp. 35–42, doi: 10.1515/bgeo-2016-0013.
29. R Core Team (2019) *A Language and Environment for Statistical Computing*. Vienna. Available at: <https://www.r-project.org/>.
30. RADECKI-PAWLIK, A., VOICU, R., PLESIŃSKI, K., GAJDA, G., RADECKI-PAWLIK, B., VOICU, L. & KSIĄŻEK, L. (2019) Difficulties with existing fish passes and their renovation. The pool fish pass on Dłubnia River in Krakow. *Acta Scientiarum Polonorum Formatio Circumiectus* 18 (2), pp. 109–119, doi: 10.15576/asp.fc/2018.18.2.109.
31. RĂDOANE, M., CIAGLIC, V. & RĂDOANE, N. (2010) Hydro-power impact on the ice jam formation on the upper Bistrița River, Romania. *Cold Regions Science and Technology* 60(3), pp. 193–204, doi: 10.1016/j.coldregions.2009.10.006.
32. REIMNITZ, E. (2002) Interaction of river discharge with sea ice in proximity of Arctic Deltas: A review. *Polarforschung* 70, pp. 123–134, doi: 10.2312/polarforschung.70.123.
33. ROGERS, W.E., THOMSON, J., SHEN, H., DOBLE, M., WADHAMS, P. & CHENG, S. (2016) Dissipation of wind waves by pancake and frazil ice in the autumn Beaufort Sea. *Journal of Geophysical Research: Oceans* 121(11), pp. 7991–8007, doi: 10.1002/2016JC012251.
34. RStudio Team (2019) *RStudio: Integrated Development for R*. Boston, MA.
35. SAFTA, C., PETICA, C.C. & MĂNDERA, L. (2018) Froude versus froude in fish ladder design. *Annals of the Academy of Romanian Scientists, Series on Engineering Sciences* 10(1), pp. 93–105.
36. SCHILT, C.R. (2007) Developing fish passage and protection at hydropower dams. *Applied Animal Behaviour Science* 104(3–4), pp. 295–325, doi: 10.1016/j.applanim.2006.09.004.
37. SCHINDELIN, J. et al. (2012) Fiji: An open-source platform for biological-image analysis. *Nature Methods* 9(7), pp. 676–682, doi: 10.1038/nmeth.2019.
38. SHAPIRO, S.S. & WILK, M.B. (1965) An analysis of variance test for normality (complete samples). *Biometrika* 52(3/4), 591, doi: 10.2307/2333709.
39. SHELARE, S.D., AGLAWE, K.R., WAGHMARE, S.N. & BELKHODE, P.N. (2021) Advances in water sample collections with a drone – A review. *Materials Today: Proceedings* 47(14), pp. 4490–4494, doi: 10.1016/j.matpr.2021.05.327.
40. SHI, X., KYNARD, B., LIU, D., QIAO, Y. & CHEN, Q. (2015) Development of fish passage in China. *Fisheries* 40(4), pp. 161–169, doi: 10.1080/03632415.2015.1017634.
41. SONG, C., OMALLEY, A., ROY, S.G., BARBER, B.L., ZYDLEWSKI, J. & MO, W. (2019) Managing dams for energy and fish tradeoffs: What does a win-win solution take? *Science of the Total Environment* 669, pp. 833–843, doi: 10.1016/j.scitotenv.2019.03.042.
42. STAMOU, A.I., MITSOPOULOS, G., RUTSCHMANN, P. & BUI, M.D. (2018) Verification of a 3D CFD model for vertical slot fish-passes. *Environmental Fluid Mechanics* 18(6), pp. 1435–1461, doi: 10.1007/s10652-018-9602-z.
43. STICKLER, M., ALFREDSEN, K., LINNANSAARI, T. & FJELDSTAD, H.-P. (2010) The influence of dynamic ice formation on hydraulic heterogeneity in steep streams. *River Research and Applications* 26(9), pp. 1187–1197, doi: 10.1002/rra.1331.
44. SVENSSON, U. & OMSTEDT, A. (1998) Numerical simulations of frazil ice dynamics in the upper layers of the ocean. *Cold Regions Science and Technology* 28(1), pp. 29–44, doi: 10.1016/S0165-232X(98)00011-1.
45. TINEVEZ, J.-Y., PERRY, N., SCHINDELIN, J., HOOPES, G.M., REYNOLDS, G.D., LAPLANTINE, E., BEDNAREK, S.Y., SHORTE, S.L. & ELICEIRI, K.W. (2017) TrackMate: An open and extensible platform for single-particle tracking. *Methods* 115, pp. 80–90, doi: 10.1016/j.ymeth.2016.09.016.
46. ZHANG, X., ZHOU, Y., JIN, J., WANG, Y., FAN, M., WANG, N. & ZHANG, Y. (2021) ICENETv2: A fine-grained river ice semantic segmentation network based on UAV images. *Remote Sensing* 13(4), 633, doi: 10.3390/rs13040633.

Cite as: Błotnicki, J., Gruszczynski, M., Jarzembowski, P., Popczyk, M. (2023) Application of close-range remote sensing for automatic identification of ice jams in rivers in the area of the inlet to the fishway. *Scientific Journals of the Maritime University of Szczecin, Zeszyty Naukowe Akademii Morskiej w Szczecinie* 75 (147), 97–106.

Supporting Materials

Table S1. Data showing track displacement, track speed, total distance, confinement ratio, and mean directional change rate obtained from the TrackMate plugin

Track ID	Track displacement	Track speed [m·s ⁻¹]	Total distance traveled	Confinement ratio	Mean directional change rate	Track ID	Track displacement	Track speed [m·s ⁻¹]	Total distance traveled	Confinement ratio	Mean directional change rate
6	3.939	0.614	4.018	0.980	0.247	63	3.794	0.592	4.040	0.939	0.441
7	4.590	0.716	4.679	0.981	0.255	64	4.076	0.636	4.244	0.960	0.384
8	4.551	0.710	4.823	0.944	0.489	65	4.001	0.624	4.132	0.968	0.331
9	4.438	0.692	4.930	0.900	0.586	67	3.781	0.590	3.935	0.961	0.340
10	3.376	0.527	4.472	0.755	0.854	68	3.746	0.584	3.845	0.974	0.286
12	4.284	0.668	4.340	0.987	0.199	69	3.740	0.584	4.528	0.826	0.729
13	3.845	0.600	3.938	0.976	0.278	70	3.809	0.594	4.140	0.920	0.599
16	4.326	0.675	6.240	0.693	1.005	71	3.880	0.605	3.974	0.976	0.269
17	4.518	0.705	4.588	0.985	0.215	74	3.675	0.573	3.815	0.963	0.343
19	4.131	0.645	4.266	0.968	0.307	76	3.089	0.482	3.198	0.966	0.329
21	3.564	0.556	3.659	0.974	0.292	77	3.691	0.576	4.089	0.903	0.643
23	4.323	0.674	4.379	0.987	0.205	79	3.633	0.567	3.751	0.968	0.311
24	4.610	0.719	4.664	0.988	0.198	80	3.657	0.570	3.721	0.983	0.222
26	3.262	0.509	3.323	0.982	0.241	81	3.569	0.557	3.844	0.929	0.535
27	4.398	0.686	4.899	0.898	0.588	84	3.552	0.554	3.635	0.977	0.264
28	3.865	0.603	4.174	0.926	0.511	85	3.591	0.560	4.105	0.875	0.750
31	3.904	0.609	3.978	0.981	0.238	86	3.510	0.548	3.653	0.961	0.359
32	4.265	0.665	4.366	0.977	0.245	87	3.521	0.549	3.955	0.890	0.591
33	4.225	0.659	4.564	0.926	0.519	88	3.323	0.518	3.366	0.987	0.178
34	3.810	0.594	4.074	0.935	0.532	90	3.078	0.480	3.154	0.976	0.257
35	3.681	0.574	3.755	0.980	0.250	92	3.513	0.548	3.783	0.929	0.476
37	4.047	0.631	5.535	0.731	0.803	94	3.464	0.540	3.693	0.938	0.515
39	4.129	0.644	4.497	0.918	0.688	95	3.409	0.532	3.668	0.929	0.495
41	4.072	0.635	5.483	0.743	0.919	99	3.262	0.509	3.590	0.909	0.509
42	3.933	0.614	4.089	0.962	0.362	100	3.348	0.522	3.415	0.980	0.233
44	4.169	0.650	4.728	0.882	0.645	102	3.272	0.510	3.467	0.944	0.422
45	4.013	0.626	4.075	0.985	0.215	107	3.377	0.527	3.682	0.917	0.485
46	3.976	0.620	4.230	0.940	0.444	111	3.330	0.520	3.408	0.977	0.263
47	4.105	0.640	4.257	0.964	0.350	112	3.398	0.530	3.545	0.959	0.383
48	4.123	0.643	4.616	0.893	0.628	114	2.968	0.463	3.140	0.945	0.441
50	3.886	0.606	4.379	0.888	0.623	116	3.309	0.516	6.137	0.539	1.251
51	3.941	0.615	4.684	0.841	0.758	118	3.244	0.506	3.637	0.892	0.546
52	4.116	0.642	4.288	0.960	0.357	120	3.326	0.519	3.946	0.843	0.731
53	3.970	0.619	4.090	0.971	0.325	121	3.582	0.559	3.640	0.984	0.206
56	3.455	0.539	3.823	0.904	0.544	123	3.347	0.522	3.549	0.943	0.437
57	3.473	0.542	3.956	0.878	0.617	127	3.630	0.566	3.780	0.960	0.356
58	3.809	0.594	4.026	0.946	0.417	128	3.642	0.568	4.752	0.766	0.912
59	3.862	0.602	3.996	0.966	0.335						